CANCER

Eradication of spontaneous malignancy by local immunotherapy

Idit Sagiv-Barfi,[1] Debra K. Czerwinski,[1] Shoshana Levy,[1] Israt S. Alam,[2] Aaron T. Mayer,[2] Sanjiv S. Gambhir,[2] Ronald Levy[1]*

It has recently become apparent that the immune system can cure cancer. In some of these strategies, the antigen targets are preidentified and therapies are custom-made against these targets. In others, antibodies are used to remove the brakes of the immune system, allowing preexisting T cells to attack cancer cells. We have used another noncustomized approach called in situ vaccination. Immunoenhancing agents are injected locally into one site of tumor, thereby triggering a T cell immune response locally that then attacks cancer throughout the body. We have used a screening strategy in which the same syngeneic tumor is implanted at two separate sites in the body. One tumor is then injected with the test agents, and the resulting immune response is detected by the regression of the distant, untreated tumor. Using this assay, the combination of unmethylated CG–enriched oligodeoxynucleotide (CpG)—a Toll-like receptor 9 (TLR9) ligand—and anti-OX40 antibody provided the most impressive results. TLRs are components of the innate immune system that recognize molecular patterns on pathogens. Low doses of CpG injected into a tumor induce the expression of OX40 on $CD4^+$ T cells in the microenvironment in mouse or human tumors. An agonistic anti-OX40 antibody can then trigger a T cell immune response, which is specific to the antigens of the injected tumor. Remarkably, this combination of a TLR ligand and an anti-OX40 antibody can cure multiple types of cancer and prevent spontaneous genetically driven cancers.

INTRODUCTION

T cells that recognize tumor antigens are present in the tumor microenvironment, and their activity is modulated through stimulatory and inhibitory receptors. Once cancer is well established, the balance between these inputs is tipped toward immunosuppression (*1*, *2*). The inhibitory signals on T cells are delivered through molecules such as cytotoxic T lymphocyte–associated protein 4 (CTLA4) and programmed cell death protein 1 (PD1) by interaction with their respective ligands expressed on cancer cells and/or antigen-presenting cells (APCs). However, these same tumor-reactive T cells express stimulatory receptors including members of the tumor necrosis factor receptor (TNFR) superfamily. Therefore, many attempts are being made to relieve the negative checkpoints on the antitumor immune response and/or to stimulate the activation pathways of the tumor-infiltrating effector T cells (T_{effs}).

Here, we conducted a preclinical screen to identify candidate immunostimulatory agents that could trigger a systemic antitumor T cell immune response when injected locally into one site of tumor. We found that Toll-like receptor 9 (TLR9) ligands induce the expression of OX40 on CD4 T cells in the tumor microenvironment. OX40 is a costimulatory molecule belonging to the TNFR superfamily, and it is expressed on both activated T_{effs} and regulatory T cells (T_{regs}). OX40 signaling can promote T_{eff} activation and inhibit T_{reg} function.

The addition of an agonistic anti-OX40 antibody can then provide a synergistic stimulus to elicit an antitumor immune response that cures distant sites of established tumors. This combination of TLR9 ligand and anti-OX40 antibody can even treat spontaneous breast cancers, overcoming the effect of a powerful oncogene. This in situ vaccine maneuver is safe because it uses low doses of the immunoenhancing agents and practical because the therapy can be applied to many forms of cancer without prior knowledge of their unique tumor antigens.

RESULTS

In situ vaccination with a TLR9 ligand induces the expression of OX40 on intratumoral CD4 T cells

TLRs are known to signal the activation of a variety of cells of the innate and adaptive immune system. To exploit this for cancer therapy, we subcutaneously implanted a tumor into syngeneic mice, and after the tumor had become established, we injected a CpG oligodeoxynucleotide—a ligand for TLR9—into the tumor nodule. We then analyzed the intratumoral T cells for their expression of inhibitory and activation markers. Before treatment, we observed that OX40 was expressed on CD4 cells in the tumor microenvironment (Fig. 1A, top) and that this was restricted mainly to the T_{regs}, as has been previously reported (*3*–*5*) (Fig. 1B, top). After intratumoral injection of CpG, there was up-regulation of OX40 on CD4 T cells (Fig. 1A, middle), mostly among the effector CD4 cells that greatly outnumber the T_{regs} (Fig. 1, A and B, bottom). This inductive effect was specific to the activating receptor OX40 and did not occur for inhibitory T cell checkpoint targets such as CTLA4 and PD1 (fig. S1A). Moreover, this OX40 up-regulation on CD4 cells also occurred in a patient with follicular lymphoma that had been treated with low-dose radiation and intratumoral injection of CpG (Fig. 1C) and in tumor-infiltrating cell populations from lymphoma patients' samples that were exposed to CpG in vitro (Fig. 1, D and E, and fig. S2). In these human cases, the enhancement of OX40 expression was observed on both T_{effs} and T_{regs} (Fig. 1D). All of these changes occurred only in the tumor that was injected with CpG and not in the tumor at the untreated site (fig. S1B).

CpG induces OX40 as revealed by in vivo imaging

The enhancement of OX40 expression by intratumoral injection of CpG could be visualized in mice by whole-body small-animal positron emission tomography (PET) imaging after tail-vein administration

[1]Division of Oncology, Department of Medicine, Stanford University, Stanford, CA 94305, USA. [2]Department of Radiology, Molecular Imaging Program at Stanford (MIPS), Stanford University, Stanford, CA 94305, USA.
*Corresponding author. Email: levy@stanford.edu

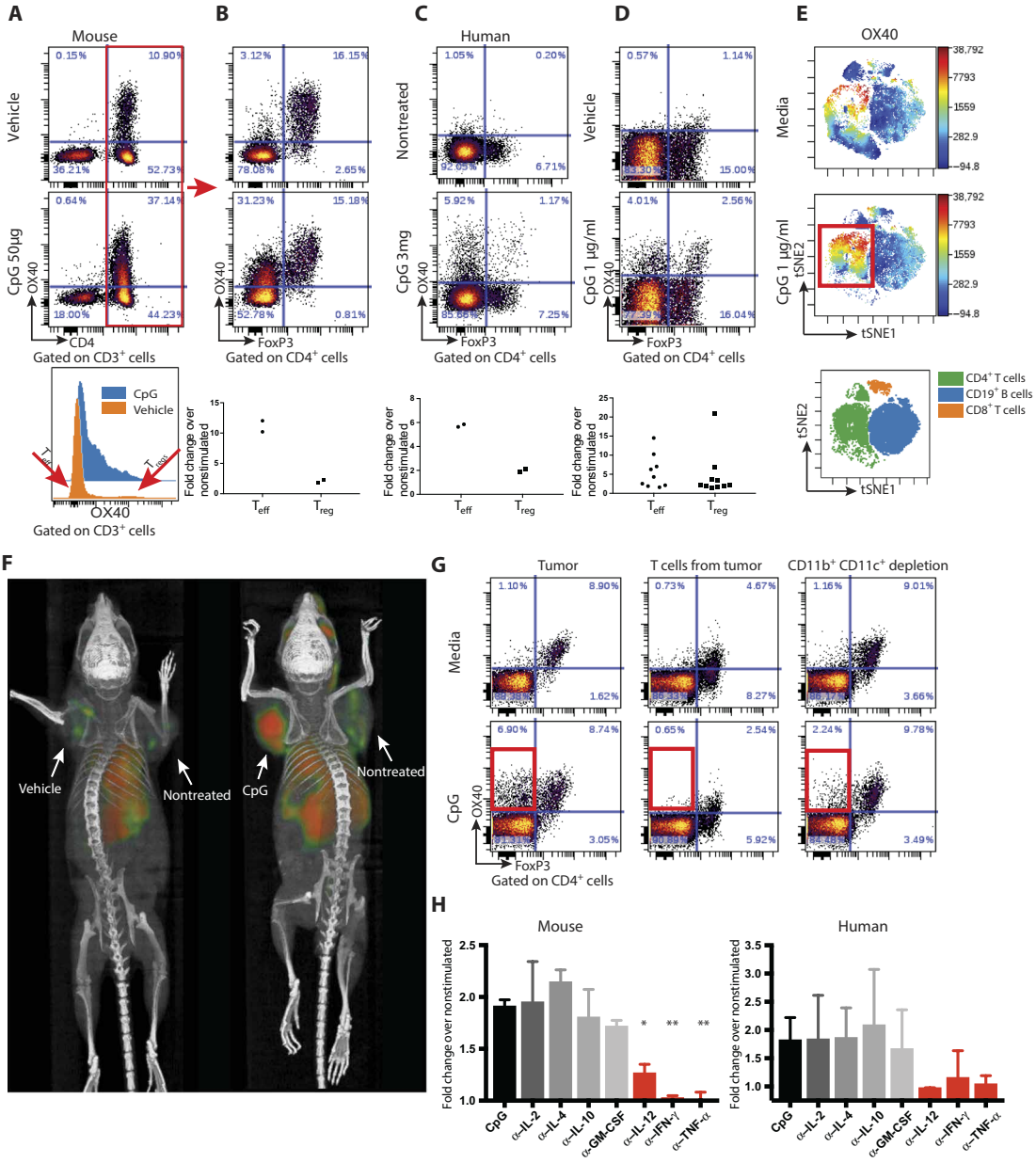

Fig. 1. CpG induces the expression of OX40 on CD4 T cells. (**A**) A20 tumor–bearing mice were treated either with vehicle (top) or CpG (middle). Forty-eight hours later, tumors were excised and a single-cell suspension was stained and analyzed by flow cytometry. (**B**) OX40 expression within the $CD3^+CD4^+$ subset was separately analyzed for FoxP3-negative [effector T cell (T_{eff})] and FoxP3-positive [regulatory T cell (T_{reg})] subsets. Fold changes of $OX40^+$ cells were calculated according to their frequencies in the vehicle versus CpG treatment ($n = 2$). (**C**) Fine needle aspirates from CpG-injected and noninjected tumors of a follicular lymphoma patient were obtained 22 hours after treatment. Fluorescence-activated cell sorting (FACS) plots of OX40 expression within the $CD4^+$ subset after a 24-hour rest in media. Top: Nontreated lesion. Bottom: CpG-treated site ($n = 2$). (**D**) Single-cell suspensions from biopsy specimens of human lymphoma (five mantle cell lymphomas and five follicular lymphomas) were exposed in vitro to CpG for 48 hours and analyzed for OX40 expression as in (B). (**E**) CpG-stimulated human lymphoma–infiltrating $CD4^+$ T cells, $CD8^+$ T cells, and $CD19^+$ B cells were gated and visualized in tSNE (t-Distributed Stochastic Neighbor Embedding) space using Cytobank software. The viSNE map shows the location of each $CD4^+$, $CD19^+$, and $CD8^+$ cell population (green, blue, and orange, respectively; bottom). Cells in the viSNE maps were colored according to the intensity of OX40 expression. CpG up-regulation of OX40 expression on a subset of $CD4^+$ T cells is highlighted by a red box. (**F**) BALB/c mice were implanted subcutaneously with A20 lymphoma cells (5×10^6) on both the right and left shoulders. When tumors reached between 0.7 and 1 cm in the largest diameter (typically on days 8 to 9 after inoculation), phosphate-buffered saline and CpG (50 μg) were injected into one tumor site (left tumor). Sixteen hours later, ^{64}Cu-DOTA-OX40 was administered intravenously via the tail vein. Positron emission tomography imaging of mice was performed 40 hours after in situ treatment. Left: Vehicle-treated. Right: CpG-treated. These images are representative of six mice per group. (**G**) Fresh A20 tumors were excised from animals (typically 5 to 6 days after inoculation), and either whole tumors (left), T cells purified from the tumor (middle), or whole tumor depleted of CD11b- and CD11c-expressing cells (right) were treated for 48 hours with media (top) or CpG (bottom) and were analyzed for their expression of OX40 by flow cytometry. (**H**) Left: A20 tumors were excised as in (F). Right: Single-cell suspensions from biopsy specimens of human follicular lymphoma. Tumors were treated for 48 hours with media and CpG with or without antibodies (1 μg/ml) to interleukin-2 (IL-2), IL-4, IL-10, granulocyte-macrophage colony-stimulating factor (GM-CSF), IL-12, interferon-γ (IFN-γ), or tumor necrosis factor–α (TNF-α) and were analyzed for their expression of OX40 by flow cytometry. α–IL-12, $^*P = 0.0144$; α–IFN-γ, $^{**}P = 0.0032$; α–TNF-α, $^{**}P = 0.008$, unpaired *t* test, either depleting antibody versus CpG alone.

of an anti-OX40 antibody labeled with ^{64}Cu (Fig. 1F). Remarkably, the systemically injected antibody revealed that OX40 was induced in the microenvironment of the injected tumor, as opposed to a second noninjected tumor site in the same animal. This result indicates that the effect of CpG at this low dose to up-regulate OX40 expression is predominately local.

CpG induces cytokine secretion by myeloid cells which in turn induces OX40 expression on T cells

Purified tumor-infiltrating T cells do not up-regulate OX40 when exposed to CpG in vitro (Fig. 1G). The T cells within whole tumor cell populations similarly fail to up-regulate OX40 after depletion of macrophages and dendritic cells (Fig. 1G). From these results, we conclude that myeloid-derived cells communicate the CpG signal to T cells. Therefore, we tested for the role of several cytokines in this cellular cross-talk. In human and mice tumors, antibody neutralization of interleukin-12 (IL-12), interferon-γ (IFN-γ), and TNF-α each prevented the CpG-induced up-regulation of OX40 on T cells in these tumor cell populations (Fig. 1H). In contrast, neutralization of IL-2, IL-4, IL-10, and granulocyte-macrophage colony-stimulating factor (GM-CSF) had no effect (fig. S3).

In situ vaccination with a TLR ligand and anti-OX40 antibody induces T cell immune responses that cure established cancers

On the basis of the results above, we hypothesized that an agonistic anti-OX40 antibody could augment CpG treatment and help to induce antitumor immune responses. To test this hypothesis, we implanted mice with A20 B cell lymphoma tumors at two different sites in the body, allowed the tumors to become established, and then injected a TLR agonist together with a checkpoint antibody into only one tumor site (Fig. 2A). The animals were then monitored for tumor growth at both the injected and the distant sites (Fig. 2B). The tumors of vehicle-treated mice grew progressively at both sites. CpG caused complete regression of tumors at the local injected site but had only a slight delay in growth of the distant nontreated tumor. The anti-OX40 antibody alone induced a slight delay in growth of both the treated and nontreated tumors. However, the combination of CpG and anti-OX40 resulted in complete regression of both injected and noninjected tumors. Consistent with the time needed to induce an adaptive T cell response, the kinetics of regression at the two sites was different, with the distant site following the local site by several days (fig. S1C). Tumor regressions in response to the combined treatment were long-lasting and led to cure of most of the mice (Fig. 2B, bottom).

The systemic antitumor response required the presence of both $CD4^+$ and $CD8^+$ T cells because mice treated with the corresponding depleting antibodies were unable to control tumor growth (Fig. 2C). $CD8^+$ T cells derived from mice treated with both CpG and anti-OX40 antibody responded to tumor cells in vitro as measured by IFN-γ production (Fig. 2D). $CD4^+$ T cells from mice treated by the combination also responded to tumors in vitro but with a lesser magnitude (fig. S4). Immediately after CpG and anti-OX40 injection, the proportion of the CD4 effector/memory T cell subset increased at the treated site. Twenty-four hours later, this subset increased in the spleen, and 5 days later, the same occurred at the distant, nontreated site (fig. S5).

Distant tumors occasionally did recur in mice treated with the effective combination (3 of 90 mice), and interestingly, these late recurring tumors were sensitive to retreatment by anti-OX40 and CpG (fig. S6). An alternative TLR agonist, resiquimod (R848), a ligand for TLR7/8, in combination with anti-OX40 induced a similar systemic antitumor immune response (fig. S7A). Anti-OX40 antibody was especially effective compared to other immune checkpoint antibodies, such as anti-PD1 and anti–PDL1 (programmed death-ligand 1) (fig. S7B), which delayed tumor growth in the nontreated site but were not curative.

In situ vaccination with CpG and anti-OX40 was effective not only against lymphoma but also against tumors of a variety of histologic types, such as breast carcinoma (4T1), colon cancer (CT26), and melanoma (B16-F10) (fig. S8, A to C). In all these tumor models, the systemic therapeutic effects were induced by extremely low doses of both the CpG (typically 50 μg) and the anti-OX40 antibody (typically 8 μg) or even lower (fig. S9). However, the TLR agonist worked best when it was injected directly into the tumor, consistent with its action to up-regulate the OX40 target in the T cells of the tumor microenvironment. Similar systemic effects were obtained when the OX40 antibody was given systemically, rather than into the tumor, but at higher doses (fig. S10).

In situ vaccination protects animals genetically prone to spontaneous breast cancers

Female FVB/N-Tg(MMTV-PyVT)634Mul/J mice (also known as PyVT/PyMT) develop highly invasive mammary ductal carcinomas that give rise to a high frequency of lung metastases (*6*). By 6 to 7 weeks of age, all female carriers develop the first palpable mammary tumor (*7*), and eventually, tumors develop in all of their 10 mammary fat pads. This provided an opportunity for therapeutic intervention in a spontaneous tumor model where the site of tumor development is known and accessible for in situ vaccination.

Young mice were observed, and as their first tumor reached 50 to 75 mm^3, we injected it with CpG and anti-OX40 antibody (Fig. 3A). In some cases, a second tumor was present at the beginning of therapy, and in these mice with coincident tumors, treatment at a single tumor site with CpG and anti-OX40 led to significant retardation of growth of the contralateral tumor (Fig. 3B), establishing the combination as a therapy for established and disseminating tumors. The injected and the noninjected tumors regressed, and remarkably, the treated mice were protected against the occurrence of independently arising tumors in their other mammary glands (Fig. 3C). The treated mice had significantly lower eventual total tumor burdens (Fig. 3, C and D) and developed far fewer lung metastases (Fig. 3E). This in situ vaccination with CpG and anti-OX40 not only caused tumor regression and reduced tumor incidence but also had a major effect on the survival of these cancer-prone mice (Fig. 3F). After CpG and anti-OX40 treatment, these mice developed antitumor CD8 T cells in their spleens as indicated by their ability to produce IFN-γ when exposed in vitro to autologous tumor cells from the noninjected tumor site (Fig. 3G). These results establish that the antitumor immune response was elicited against tumor antigens shared by all the independently arising tumors in these mice, rather than antigens unique to the injected tumor, and accounted for the impressive therapeutic effects seen.

Therapeutic effect of in situ vaccination is antigen-specific and triggered at the site of local injection

The results of cross-protection against independently arising tumors in the spontaneous breast cancer model raise the question of antigen specificity. We approached this question using two different tumors that are antigenically distinct. Mice cured by in situ vaccination of the A20 lymphoma were immune to rechallenge with the same tumor (A20) but not to a different tumor (CT26) (fig. S11). Conversely, mice cured of the CT26 tumor were immune to rechallenge with CT26 but not with A20. Therefore, these two tumors are antigenically distinct.

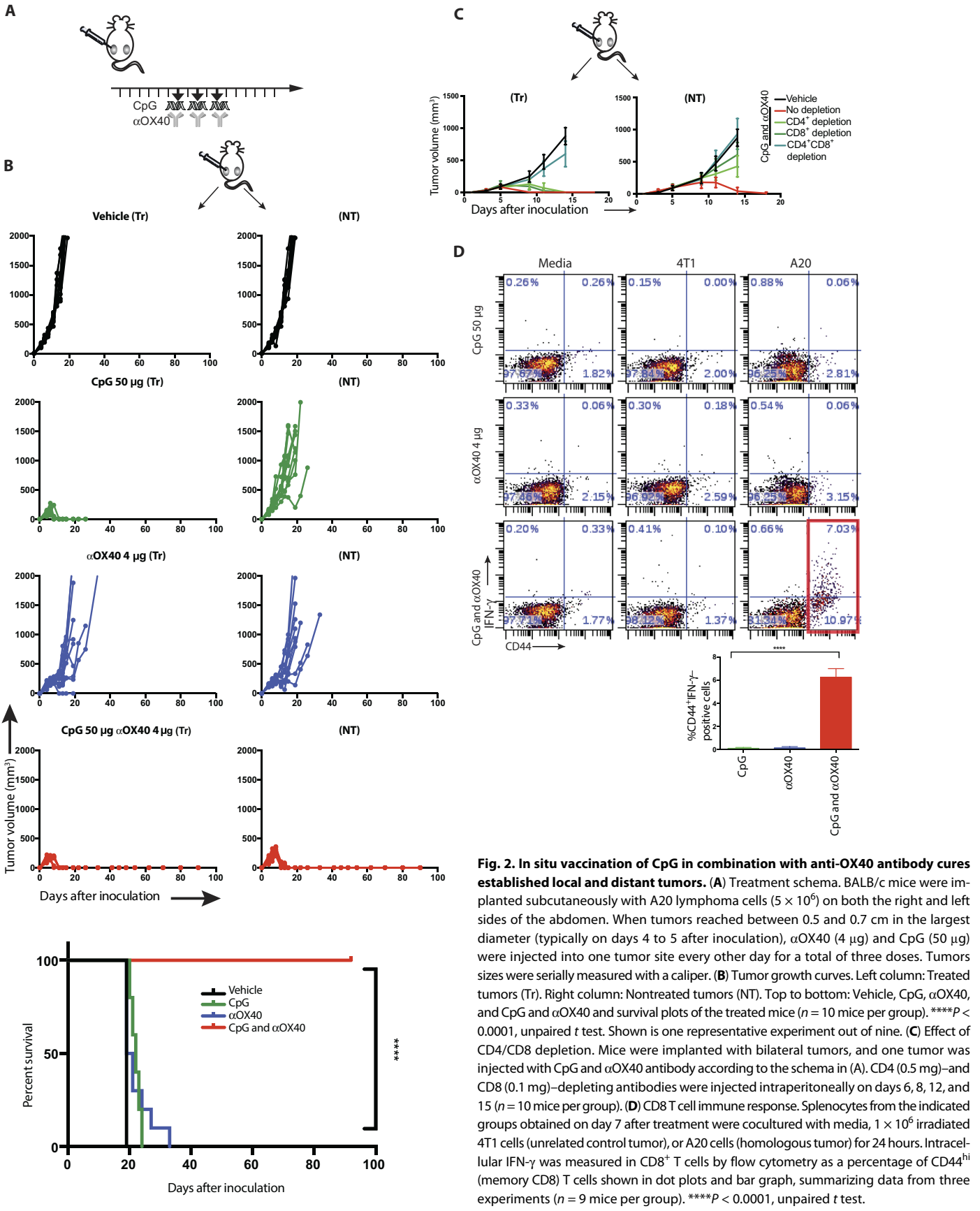

Fig. 2. In situ vaccination of CpG in combination with anti-OX40 antibody cures established local and distant tumors. (**A**) Treatment schema. BALB/c mice were implanted subcutaneously with A20 lymphoma cells (5×10^6) on both the right and left sides of the abdomen. When tumors reached between 0.5 and 0.7 cm in the largest diameter (typically on days 4 to 5 after inoculation), αOX40 (4 μg) and CpG (50 μg) were injected into one tumor site every other day for a total of three doses. Tumors sizes were serially measured with a caliper. (**B**) Tumor growth curves. Left column: Treated tumors (Tr). Right column: Nontreated tumors (NT). Top to bottom: Vehicle, CpG, αOX40, and CpG and αOX40 and survival plots of the treated mice ($n = 10$ mice per group). ****$P <$ 0.0001, unpaired t test. Shown is one representative experiment out of nine. (**C**) Effect of CD4/CD8 depletion. Mice were implanted with bilateral tumors, and one tumor was injected with CpG and αOX40 antibody according to the schema in (A). CD4 (0.5 mg)–and CD8 (0.1 mg)–depleting antibodies were injected intraperitoneally on days 6, 8, 12, and 15 ($n = 10$ mice per group). (**D**) CD8 T cell immune response. Splenocytes from the indicated groups obtained on day 7 after treatment were cocultured with media, 1×10^6 irradiated 4T1 cells (unrelated control tumor), or A20 cells (homologous tumor) for 24 hours. Intracellular IFN-γ was measured in $CD8^+$ T cells by flow cytometry as a percentage of $CD44^{hi}$ (memory CD8) T cells shown in dot plots and bar graph, summarizing data from three experiments ($n = 9$ mice per group). ****$P < 0.0001$, unpaired t test.

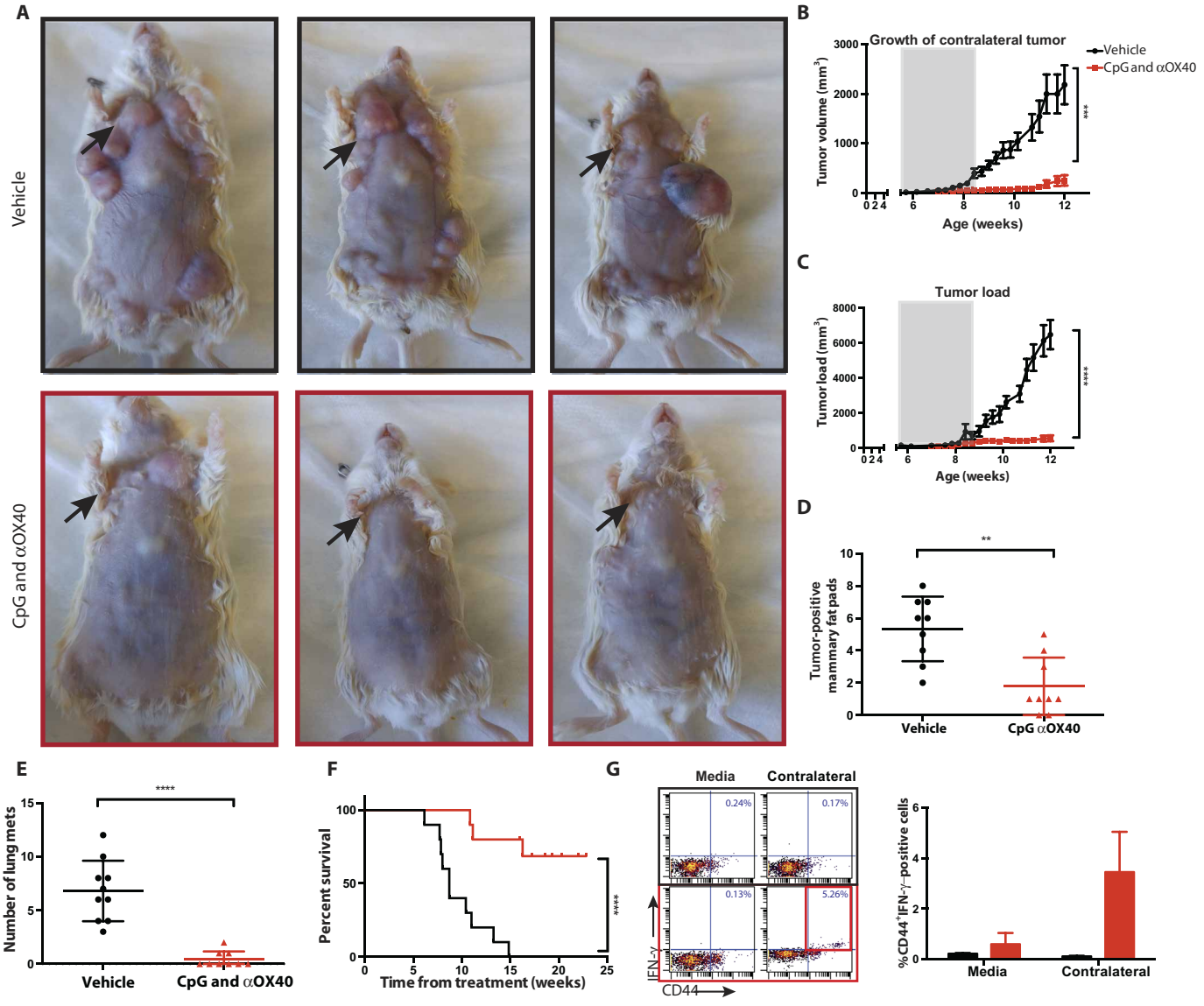

Fig. 3. In situ vaccination with CpG and anti-OX40 is therapeutic in a spontaneous tumor model. (**A**) MMTV-PyMT transgenic female mice were injected into the first arising tumor (black arrow) with either vehicle (top) or with CpG and αOX40 (bottom); pictures were taken on day 80. (**B**) CpG and αOX40 decrease the tumor size of a nontreated contralateral tumor. Growth curves represent the volume of a contralateral (untreated) tumor in mice that had two palpable tumors at the beginning of treatment. Mice treated by in situ vaccination (red; $n = 6$) or vehicle (black; $n = 6$). ***$P = 0.0008$, unpaired t test. (**C**) CpG and αOX40 decrease the total tumor load. Growth curves represent the sum of the volume of 10 tumors from the different fat pads of each mouse, measured with calipers ($n = 10$ mice per group), and the window of treatment is indicated by the gray bar. ****$P < 0.0001$, unpaired t test. (**D**) Time-matched quantification of the number of tumor-positive mammary fat pads. **$P = 0.011$, unpaired t test ($n = 9$ mice per group). (**E**) Mice were sacrificed at the age of 80 days, and lungs were excised and analyzed ex vivo for the number of metastases (mets). ****$P < 0.0001$, unpaired t test ($n = 10$ mice from vehicle-treated group; $n = 9$ mice with CpG and αOX40). (**F**) Survival plots of the treated mice. ****$P < 0.0001$. Data are means ± SEM ($n = 10$ mice per group). (**G**) CD8 T cell immune response. Splenocytes from the indicated groups obtained on days 7 to 15 after treatment were cocultured for 24 hours with either media or 1×10^6 irradiated tumor cells taken from an independent contralateral site on the body. Intracellular IFN-γ was measured in $CD8^+$ T cells by flow cytometry as shown in dot plots and bar graph, summarizing data as a percentage of $CD44^{hi}$ (memory CD8) T cells ($n = 3$ mice per group).

To further demonstrate the specificity of the antitumor response, we implanted tumors into mice at three different body sites: two with the A20 and one with CT26 (Fig. 4A). One A20 tumor site was then injected with CpG and anti-OX40 antibody. Both A20 tumors, the injected one and the noninjected one, regressed but the unrelated CT26 tumor continued to grow (Fig. 4A). In a reciprocal experiment, we injected mice with two CT26 tumors and one A20 tumor and treated one CT26 tumor. Once again, only the homologous distant tumors (in this case, CT26) regressed but not the unrelated A20 tumor (Fig. 4B). This result confirmed that the immune response induced by the therapy was tumor-specific. Furthermore, it demonstrated that in situ vaccination with these low doses of agents works by triggering an immune response in the microenvironment of the injected site rather than by diffusion of the injected agents to systemic sites.

Naturally arising tumors can show intratumoral antigenic heterogeneity. To test whether CpG and anti-OX40 treatment can trigger an

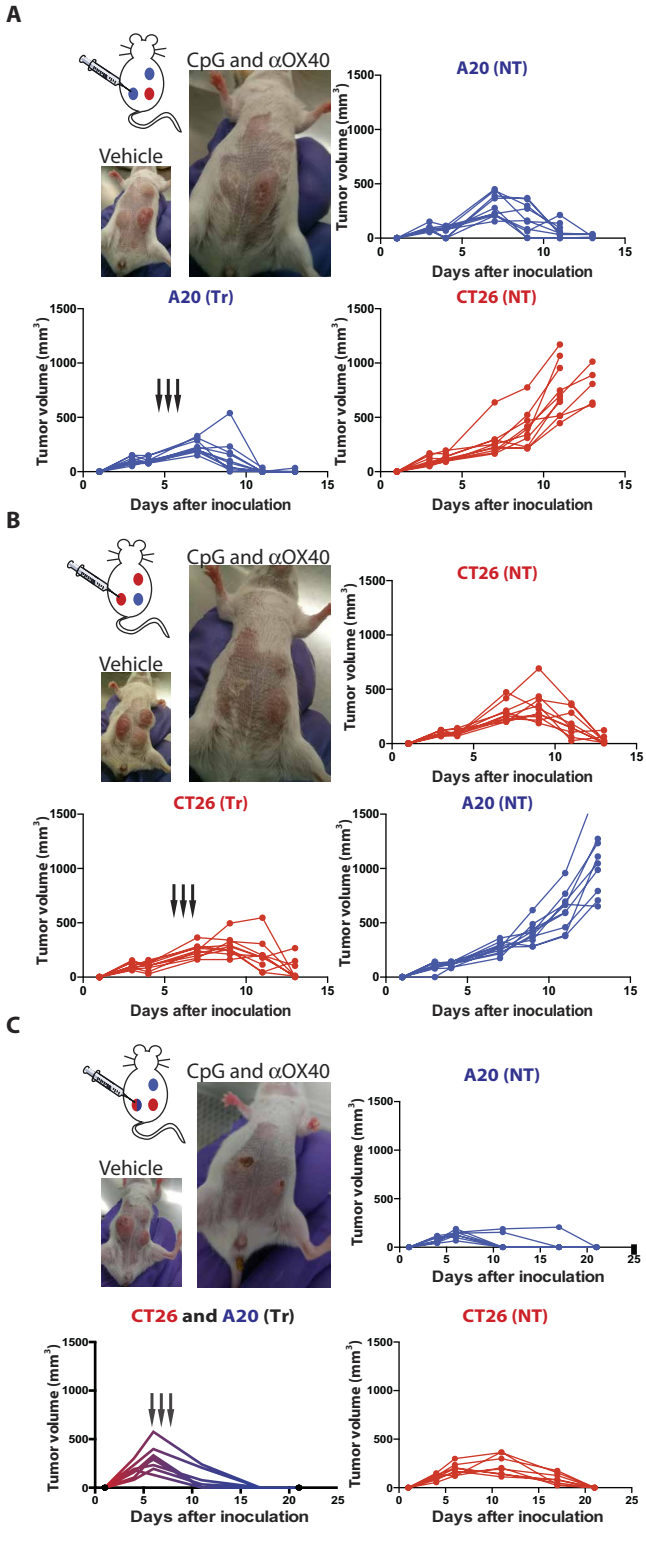

Fig. 4. Immunizing effects of intratumoral CpG and anti-OX40 are local and tumor-specific. (**A**) Three-tumor model. Each mouse was challenged with three tumors, two of them A20 lymphoma (blue) and one CT26 colon cancer (red). Mice were treated at the indicated times (black arrows). Tumor growth curves of the treated tumor (bottom left), the homologous nontreated A20 tumor (top right), and the heterologous CT26 tumor (bottom right). Photos of a representative mouse at day 11 after tumor challenge from the vehicle-treated group and from the group with A20 tumors treated with intratumoral CpG and αOX40 (n = 10 mice per group) are shown. (**B**) Reciprocal three-tumor model with two CT26 tumors and one A20 tumor. Treatment was given to one CT26 tumor, and growth curves are shown for the treated CT26 tumor site (bottom right), the nontreated homologous CT26 tumor site (top right), and the heterologous A20 tumor (bottom right). Photos of a representative mouse from this experiment (n = 10 mice per group) are shown. (**C**) Mixed three-tumor model. Each mouse was challenged with three tumors: one A20 (blue, top right abdomen), one CT26 (red, bottom right abdomen), and one mixture of A20 and CT26 tumor cells (blue and red gradient, left abdomen). Mice were treated only in the mixed tumor at the indicated times (black arrows). Tumor growth curves of the treated tumor (bottom left), the nontreated A20 tumor (top right), and the nontreated CT26 tumor (bottom right). Photos of a representative mouse at day 11 after tumor challenge from the vehicle-treated group (top) and at day 17 from the intratumoral CpG and αOX40 (n = 8 mice per group) are shown.

immune response against multiple different tumor antigens at the same time, we injected mice with a mixture of A20 and CT26 tumor cells at one site, treated that site with local CpG and anti-OX40 antibody, and monitored two additional sites of tumor containing each of the single tumor cells (A20 and CT26, respectively). In situ vaccination of the mixed tumor site simultaneously induced immune responses protective of each of the respective other two pure tumor sites (Fig. 4C). These results demonstrate the power of in situ vaccination to simultaneously immunize against a panoply of different tumor antigens.

Fc competency is required for efficacy of the anti-OX40 antibody

OX40 is expressed on both intratumoral FoxP3$^+$ T_{regs} and activated T_{effs} (Fig. 1B). The immunoenhancing activity of the anti-OX40 antibody could therefore be mediated by inhibition/depletion of T_{regs}, by stimulation of T_{effs}, or by a combination of both. We tested the anti-OX40 T_{reg} depletion hypothesis by replacing it with an antibody against folate receptor 4 (FR4), a T_{reg}-depleting agent (fig. S12A) (*8*). T_{regs} were partially depleted (43% reduction) by the anti-FR4 in combination with CpG, but no distant therapeutic effect occurred (Fig. 5A). We further investigated this question using mice genetically engineered to express diphtheria toxin under the FoxP3 promoter (*9*, *10*). Injection of diphtheria toxin led to complete T_{reg} depletion in these mice (fig. S12B). However, when combined with intratumoral CpG, no distant therapeutic effect was observed (Fig. 5B). As others have shown, stimulation of T_{regs} through OX40 can impair their function (*4*, *11*, *12*), which we confirm here (fig. S13, A and B). Therefore, we conclude that T_{reg} stimulatory impairment but not depletion is involved in the mechanism of therapeutic synergy with CpG. To dissect the mechanism of these potent therapeutic effects, we compared two different forms of the anti-OX40 antibody that differ in their ability to bind to CD16: the activating Fc receptor on natural killer (NK) cells and macrophages. When used in combination with CpG, the native, Fc-competent version of anti-OX40 antibody induced systemic antitumor immunity, whereas the Fc-mutant version did not (Fig. 5A). We repeated the in situ vaccination experiment in mice deficient in the Fc common γ chain, a component of the activating Fc γ receptors I, III, and IV (*13*). Once again, in the absence of Fc receptor interaction, this time at the level of the host, the effect of in situ vaccination with CpG and anti-OX40 antibody was lost (fig. S14). These results could implicate ADCC (antibody-dependent cellular cytotoxicity) function of the antibody or alternatively an Fc-dependent agonistic action of the anti-OX40 antibody (*14*, *15*).

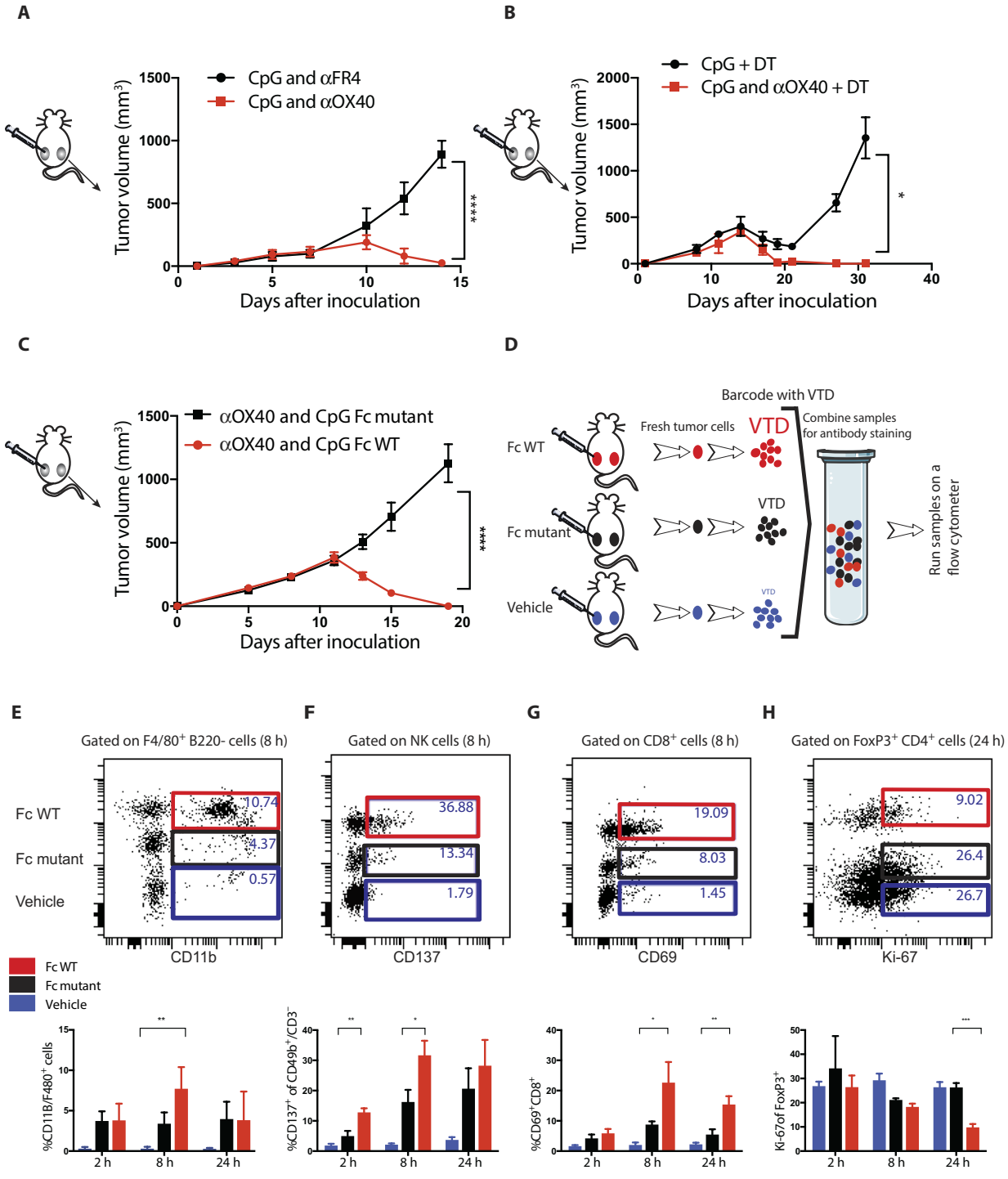

Fig. 5. A competent Fc is required for the antitumor immune response. (**A** and **B**) Effect of T_{reg} depletion. (A) Tumors were implanted according to the schema in Fig. 2A. Mice were treated with either CpG and anti–folate receptor 4 (FR4) antibody (15 μg) or CpG and αOX40 as described in Fig. 2A, and the NT was measured over time. ****$P <$ 0.0001, unpaired *t* test ($n = 10$ mice per group). (B) DEREG mice were implanted with B16-F10 melanoma cells (0.05×10^6) on both the right and left sides of the abdomen. Diphtheria toxin (DT; 1 μg) was injected intraperitoneally on days 1, 2, 7, and 14. CpG or combination of CpG and anti-OX40 was given on days 7, 9, and 11. The NT was measured over time. *$P = 0.0495$, unpaired *t* test ($n = 4$ mice per group). (**C**) A20 cells were inoculated and treated as described in Fig.2A, tumor volumes were measured after treatment of CpG with either αOX40 rat immunoglobulin G1 (IgG1) (red) or αOX40 rat IgG1 Fc mutant (black). ****$P < 0.0001$, unpaired *t* test ($n = 10$ mice per group). WT, wild type. (**D**) Tumors from control and treated mice were excised at the indicated times after a single treatment, and the cell populations from the different groups were differentially labeled (barcoded) with two different levels of violet tracking dye (VTD) and mixed together, stained, and analyzed as a single sample [$n = 3$ mice per group (C to F)]. (**E** to **H**) Dot plots for single time point and bar graphs for replicates of multiple time points. (E) Number of F4/80 $CD11b^+$ myeloid cells. **$P = 0.009$ (8 h), Fc WT versus vehicle. (F) CD137 expression on natural killer (NK) cells. **$P = 0.0035$ (2 h), *$P = 0.0343$ (8 h), unpaired *t* test, Fc WT versus Fc mutant. (G) CD69 expression on $CD8^+$ T cells. *$P =$ 0.025 (8 h), **$P = 0.0064$ (24 h), unpaired *t* test, Fc WT versus Fc mutant. (H) T_{reg} cell proliferation. ***$P = 0.0003$ (24 h), unpaired *t* test, Fc WT versus Fc mutant.

Therefore, we examined immune cells in the tumor microenvironment during the early phases of treatment with intratumoral CpG and compared the changes induced with the Fc-competent to those induced by the Fc-mutant version of the anti-OX40 antibody. Early after in situ vaccination, within 24 hours, the tumor-infiltrating cell populations from animals treated with Fc-competent or Fc-mutant antibodies were barcoded (*16*), pooled, and then costained by a panel of antibodies to identify subsets of immune cells and their activation states (Fig. 5B). The cell populations derived from the different treatment groups were then separately identified by their barcodes. In response to the anti-OX40 antibody with the native Fc, there was an increase in myeloid cell infiltration (Fig. 5C), a cell population important in the cross-talk between CpG and the T cells (see above; Fig. 1, F and G). NK cells showed an Fc-dependent up-regulation of their CD137 activation marker (Fig. 5D). In addition, the Fc-competent but not the Fc-mutant antibody induced activation of a population of CD8 T cells, as indicated by increased CD69 expression (Fig. 5E). T_{regs} were inhibited in their proliferation by comparison to those exposed to the antibody with the mutated Fc region (Fig. 5F). Neither T_{regs} nor T_{effs} were killed by the Fc-competent antibody (fig. S15). These early cellular changes occurred only in the tumor microenvironment of the treated site and were not evident at other sites throughout the mouse (fig. S1B). These results imply that anti-OX40 antibodies, in conjunction with TLR ligands, can induce therapeutic systemic antitumor immune responses by a combination of NK cell activation, T_{reg} inhibition, and T_{eff} activation, all at the treated tumor site.

DISCUSSION

We have developed a practical strategy for immunotherapy of cancer. It takes advantage of the preexisting T cell immune repertoire within the tumor microenvironment. The combination of a TLR agonist and an activating antibody against OX40 amplifies these antitumor T cells and induces their action throughout the body against tumor at nontreated sites. This in situ vaccination does not require knowledge of the tumor antigens. Potential drawbacks include reliance on adequate immune infiltrates and the availability of a suitable injectable site of tumor.

After screening a series of immune activators and checkpoint antibodies, we identified the combination of CpG oligodeoxynucleotide (TLR9 ligand) and anti-OX40 antibody to be the most potent form of in situ vaccination in multiple mouse models. TLR7/8 agonists could substitute for CpG, but checkpoint antibodies against PD1, PDL1, or CTLA4 could not substitute for anti-OX40.

The synergistic therapeutic effect between locally injected CpG and anti-OX40 antibodies is explained by the fact that CpG induced the expression of the OX40 target on $CD4^+$ T cells in the tumor microenvironment. CpG also induced OX40 in $CD4^+$ T cells in the tumor microenvironment of human lymphoma tumors, and therefore, our results are likely to translate to human cancer.

It has been reported that local intratumoral administration of CpG together with systemic antibody against IL-10R leads to rejection of the injected tumor and distant metastases (*17*, *18*). This combination was shown to deflect M2 to M1 macrophages in the tumor microenvironment (*19*). Therefore, we examined the requirement for induction of OX40 expression on CD4 T cells by CpG in our system. We found that it was dependent on cytokines secreted by myeloid cells, including IL-12, IFN-γ, or TNF-α but not IL-2, IL-4, IL-10, and GM-CSF.

The therapeutic effect at the distant sites was specific for antigens expressed by the tumor at the injected site that were shared with the tumor cells at the distant sites. This result not only established the tumor specificity of the immunization but also proved that it was the local effect of the injected agents in the tumor microenvironment rather than their systemic delivery that triggered the systemic antitumor immune response.

Autoimmune toxicities are a common complication of systemically administered immune checkpoint antibodies (*20*–*24*). In contrast, direct injection of the antibodies into the tumor at very low doses can avoid these side effects (*25*, *26*). In our experiments, in situ injection of microgram quantities of immune stimulants and checkpoint antibodies proved to be sufficient to induce the required local immune modulation, resulting in a systemic antitumor immune response.

A major challenge in tumor immunotherapy lies in breaking tumor immune tolerance. In a previous report, we showed that depletion of tumor-specific T_{regs} by the addition of anti-CTLA4 antibody was associated with enhanced antitumor efficacy (*27*). However, we find here that activating antibody against OX40 is sufficient. It is known that OX40 is expressed on both T_{regs} and T_{effs} in the tumor microenvironment, and as we now realize, OX40 can be further induced on $CD4^+$ T cells in response to CpG. Modulating both T_{effs} and T_{regs} is essential to obtain therapeutic effect (*28*–*30*). Antibodies to OX40 costimulate T_{effs} (*31*–*37*), and they also inhibit the function of T_{regs} (*12*, *27*, *38*–*40*).

Having demonstrated the potent therapeutic efficacy of in situ immunotherapy in several different transplanted tumor types, we assessed this form of therapy in a spontaneous arising tumor. The MMTV-PyMT mouse model recapitulates several of the characteristics of virulent human breast cancer, among them showing histology similarity, having loss of estrogen and progesterone receptors, and overexpressing ErbB2/Neu and cyclin D1 (*6*, *41*, *42*). Although the tumors within a mouse arise independently in different mammary glands, they all share the expression of the PyMT antigen (*43*). Injection of CpG and anti-OX40 antibody into the first tumor to occur in each mouse resulted in reduced tumor load in the other mammary fat pads and prevented lung metastases. These results demonstrate the potency of the in situ vaccine maneuver in a situation of spontaneous cancer-driven by a strong oncogene, suggesting the possibility of a direct application to human cancer. By analogy to the genetically prone mice, we can imagine administering an in situ vaccine at the site of the primary tumor before surgery in patients at high risk for the occurrence of metastatic disease and/or in patients genetically prone to develop second primary cancers, such as those with inherited mutation in the BRCA genes.

The CpG used here, SD-101, is currently being tested in patients as a single agent and in combination with other therapeutic modalities (NCT02927964, NCT02266147, NCT01745354, NCT02254772, and NCT02521870). Anti-OX40 antibody is also currently being studied in phase 1 clinical trials (NCT02559024, NCT01644968, NCT02221960, NCT02318394, NCT02274155, NCT01862900, NCT01303705, and NCT02205333). The results from our current preclinical studies provide strong rationale for combining CpG with agonistic anti-OX40 antibodies in a therapeutic format of in situ vaccination in patients with lymphoma and solid tumors. As we have shown, CpG and anti-OX40 antibodies work locally at very low doses that should provide the advantage of avoiding toxicities that occur with their systemic administration.

MATERIALS AND METHODS

Study design

Our objective was to develop a new immunotherapy for cancer by using the tumor itself as a source of antigen, of immune reactive cells and as a site for injecting immune activating agents—in situ vaccination. Our general strategy was to implant the same syngeneic tumor at two separate sites in the body of mice. One tumor was then injected with the test agents, and tumor size was measured in both the treated and nontreated sites. Using this assay for abscopal therapeutic effects, we identified the combination of unmethylated CG–enriched oligodeoxynucleotide (CpG)—a TLR9 ligand—and an agonistic antibody against OX40 as the most promising immunostimulatory regimen.

Because transplanted syngeneic tumor models lack certain aspects of naturally occurring tumors, we also studied the effects of our combination in a spontaneous model of breast cancer. This model is driven by the polyoma middle T oncogene under the control of the MMTV promoter, and the female mice develop independently arising breast cancers in all of their mammary glands between 5 and 14 weeks of age.

We observed the mice, and when their first breast cancer tumor arose, we injected it with our combination of CpG and anti-OX40 antibody. Each mouse was then monitored for the regression of simultaneously present second tumors, for the occurrence of newly arising tumors, for metastatic disease in their lungs, and for their survival. Data were analyzed by Kaplan-Meier curves with events scored as the time to reach 2 cm in the largest diameter at which time the mouse was sacrificed. Data were analyzed using the log-rank test.

We studied the mechanism of the therapy by examining the requirement for T cells and their subsets, including T_{regs}, and by the requirement for Fc function of the anti-OX40 antibody. These requirements were tested by depleting specific T cells and by substituting an Fc mutant for the native anti-OX40 antibody.

In all therapy experiments, to ensure similar tumor sizes in all treatment groups, mice were randomized only after tumors were established. To ensure statistical power, experimental groups were typically composed of 10 animals each. For each experiment, mice numbers, statistical tests, and numbers of experimental replicates are described in the figure legends. Data include all outliers. Investigators were not blinded during evaluation of the in vivo experiments. Raw data for all therapy experiments are provided in table S1.

Reagents

CpG SD-101 was provided by Dynavax Technologies. Anti-mouse CD8a (clone 2.43) and anti-mouse CD4 (clone GK1.5) antibodies were purchased from BioXCell. Anti-OX40 (CD134) monoclonal antibody (mAb) [rat immunoglobulin G1 (IgG1), clone OX86; European Collection of Cell Cultures], isotype control rat hybridoma, SFR8-B6 [American Type Culture Collection (ATCC) HB-152] were produced as ascites in severe combined immunodeficient mice by Bionexus. Fc-silent Anti-OX40 (CD134) mAb was purchased from Absolute Antibody.

The following mAbs were used for flow cytometry: CD4-PerCP (peridinin chlorophyll protein) Cy5.5, CD3-PerCP Cy5.5, or BV786; CD4-BV650, CD8a–FITC (fluorescein isothiocyanate), or APC (allophycocyanin) H7; CD44-APC, IFN-γ–PE (phycoerythrin), B220-PerCP Cy5.5, CD49b-PE CY7, CD69-BV605, CD137-PE, and ICOS (CD278)–PE Cy7; FoxP3-PE; and Ki-67–BV711. These antibodies and their isotype controls were purchased from BD Biosciences, BioLegend, or eBioscience.

Cell lines and mice

A20 B cell lymphoma, B16-F10 melanoma, and CT26 colon carcinoma lines were obtained from ATCC, and 4T1-Luc breast carcinoma cell line was a gift from the S. Strober laboratory and the C. Contag laboratory (both at Stanford University). Tumor cells were cultured in complete medium (RPMI 1640; Dulbecco's modified Eagle's medium for B16-F10; Cellgro) containing 10% fetal bovine serum (FBS; HyClone), penicillin (100 U/ml), streptomycin (100 μg/ml), and 50 μM 2-mercaptoethanol (Gibco). Cell lines were routinely tested for mycoplasma contamination.

Six- to 8-week-old female BALB/c and C57BL/6 were purchased from Charles River (www.criver.com). FVB/N-Tg(MMTV-PyVT)634Mul/J male FVB/NJ females [C57BL/6-Tg(Foxp3-DTR/EGFP)23.2Spar; also known as DEREG mice] were purchased from The Jackson Laboratory (http://jaxmice.jax.org/). Mice were housed in the Laboratory Animal Facility of the Stanford University Medical Center (Stanford, CA). All experiments were approved by the Stanford administrative panel on laboratory animal care and conducted in accordance with Stanford University animal facility guidelines.

Tumor inoculation and animal studies

A20, CT26, 4T1, and B16-F10 tumor cells (5×10^6, 0.5×10^6, 0.01×10^6, and 0.05×10^6, respectively) were injected subcutaneously at sites on both the right and left sides of the abdomen. When tumor size reached 0.5 to 0.7 cm in the largest diameter, mice were randomized to the experimental groups. CpG and anti-OX40 were injected into the tumor only on the right side of the animals in a volume of 50 μl. Tumor size was monitored on both sides of the animals with a digital caliper (Mitutoyo) every 2 to 3 days and expressed as volume (length × width × height). Mice were sacrificed when tumor size reached 1.5 cm in the largest diameter as per guidelines. All mice that developed tumors on both sides of the abdomen were included in the experiments. The investigator was not blinded to the group allocation during the experiment and/or when assessing the outcome.

4T1 tumor–challenged mice were analyzed for lung metastasis by injecting India ink through the trachea after euthanasia. Lungs were then excised, washed once in water, and fixed in Fekete's solution (100 ml of 70% alcohol, 10 ml of formalin, and 5 ml of glacial acetic acid) at room temperature. Surface metastases subsequently appeared as white nodules at the surface of black lungs and were counted under a microscope.

DEREG mice were implanted with B16-F10 tumor cells as described above. Diphtheria toxin (1 μg; Sigma-Aldrich) was injected intraperitoneally on days 1, 2, 7, and 14 after tumor implantations. CpG or combination of CpG and anti-OX40 was given on days 7, 9, and 11 after tumor implantations.

Flow cytometry

Cells were surface-stained in phosphate-buffered saline (PBS), 1% bovine serum albumin, and 0.01% sodium azide, fixed in 2% paraformaldehyde, and analyzed by flow cytometry on a FACSCalibur or LSR II (BD Biosciences). Data were stored and analyzed using Cytobank (www.cytobank.org).

Multiplex flow cytometry—fluorescent cell barcoding

Excised tumors from mice treated with an Fc-competent OX40 antibody, an Fc-silent OX40 antibody (Absolute Antibody), or saline were mechanically processed into single-cell suspensions and barcoded using three different concentrations of CellTrace Violet Proliferation

reagent (Life Technologies) ranging from 5 to 0.1 μM. Once barcoded, equal numbers of cells from each group were combined and stained with LIVE/DEAD Fixable Green Dead Cell Stain (Life Technologies) followed by antibodies against surface antigens to determine populations of interest such as tumor (B220), T cells (CD3, CD4, and CD8), and NK cells (CD56) as well as those to look at activation (CD69, CD137, and ICOS). Cells were then fixed and permeabilized (eBioscience), stained for FoxP3 (T_{regs}) and Ki-67 (proliferation), and analyzed by flow cytometry.

IFN-γ production assay

Single-cell suspensions were made from spleens of treated mice (on day 7 after treatment), and red cells were lysed with ammonium chloride and potassium buffer (Quality Biological). Splenocytes were then cocultured with 1×10^6 irradiated A20 or 4T1 cells for 24 hours at 37°C and 5% CO_2 in the presence of 0.5 μg of anti-mouse CD28mAb (BD Pharmingen). Monensin (GolgiStop; BD Biosciences) was added for the last 5 to 6 hours. Intracellular IFN-γ expression was assessed using BD Cytofix/Cytoperm Plus Kit as per the manufacturer's instructions.

Depletion of CD4 and CD8 T cells

Anti-CD4 (clone GK1.5, rat IgG2b) and anti-CD8 (clone 2.43, rat IgG2b) mAbs (BioXCell) were injected 2 days and 1 day before therapy, on the day therapy was begun, and at 5, 8, and 19 days after the beginning of therapy at a dose of 0.5 or 0.1 mg per injection for CD4 and CD8, respectively. The depletion conditions were validated by flow cytometry of blood showing specific depletion of more than 95% of each respective cell subset.

In vitro assessment of OX40 expression

Fresh tumor cells were excised from mice, processed into single-cell suspensions, and incubated for 48 hours with CpG (1 μg/ml). Cells were then stained for the surface antigens CD3, CD4, CD8, and OX40. They were then fixed and permeabilized using reagents from eBioscience, followed by FoxP3 staining. T cell isolation and depletion of T cells and CD11b- and CD11c-expressing cells from tumors used kits from Miltenyi Biotec.

Tetramer staining

PE-conjugated H-2Ld tetramer to peptide SPSYVYHQF (MuLV env gp70, 423 to 431) was purchased from ProImmune, and PE-conjugated H-2Ld tetramer to peptide IASNENMETMESSTLE (influenza nucleoprotein 365 to 380) was a gift from the M. Davis laboratory (Stanford University). Antibodies were used at 5 μg/ml, and tetramer staining was performed in fluorescence-activated cell sorting buffer for 10 min at room temperature and followed by surface staining on ice for 20 min.

Activation and suppression assay

T cell activation assay

C57BL/6 splenocytes were isolated, violet tracking dye (VTD)–labeled, and incubated in the presence of anti-CD3 antibody (0.05 μg/ml) for 72 hours with or without anti-OX40 antibodies. T cell activation and proliferation were determined by VTD dilution and the expression of the activation marker CD69.

T_{reg} suppression assay

To determine the impact of OX40 antibodies on T_{reg} activity, VTD-labeled splenic cells were cocultured with OX40–KO (knockout) T_{regs} [OX40 wild-type (WT) splenocytes/OX40 KO T_{reg} = 1:1]. Cells were cocultured in 96-well plate in the presence of anti-CD3 and anti-CD28 beads (Thermo Fisher Scientific) for 96 hours with or without anti-OX40 antibody (1 μg/ml). Proliferation of the WT-labeled T_{effs} was measured by flow cytometry and calculated by VTD dilution. T_{regs} were isolated using kits from Miltenyi Biotec.

PET imaging

PET imaging of mice was performed using the microPET/CT hybrid scanner (Inveon, Siemens). PET images were reconstructed using 2 iterations of three-dimensional ordered subset expectation maximization (3DOSEM) algorithm (12 subsets) and 18 iterations of the accelerated version of 3D-MAP (that is, FASTMAP)—matrix size of 128 × 128 × 159. Computed tomography (CT) images were acquired just before each PET scan to enable attenuation correction of the PET data set and provided an anatomic reference for the PET image. Mice were anesthetized using isoflurane gas (2.0 to 3.0% for induction and 2.0 to 2.5% for maintenance). ^{64}Cu-DOTA-OX40 (80 to 110 μCi; radiochemical purity of 99% as determined by thin-layer chromatography; and specific activity is 185 MBq/mg) was administered intravenously via the tail vein 16 hours after CpG and vehicle intratumoral injections. Static PET scans (10 min) were acquired 16 hours after intravenous administration of ^{64}Cu-DOTA-OX40 (40 hours after intratumoral injections). Once reconstructed using a 3DOSEM algorithm, PET images were coregistered with CT images to generate figures using the IRW (Inveon Research Workplace) image analysis software (version 4.0; Siemens).

Up-regulation of OX40 on CD4 T cells infiltrating human B cell tumors

Tumor samples from patients with Follicular and Mantle Cell B cell lymphoma who were part of ongoing clinical trials [Stanford International Review Board (IRB) protocols IRB-31224, IRB-36750, and IRB-5089] were available for in vitro analysis. Single-cell suspensions were incubated for either 24 or 48 hours in RPMI medium containing 5% FBS (HyClone), penicillin (100 U/ml), and streptomycin (100 μg/ml) and then stained for T cell surface antigens including CD3, CD4, CD8, and OX40. They were also fixed and permeabilized using reagents from eBioscience and then stained for FoxP3. For in vitro stimulation studies, CpG at a concentration of 1 μg/ml was added to the medium.

For response of tumor-infiltrating cells to CpG in vivo, a sample was obtained from a site of tumor that had been injected with CpG (3 mg) 24 hours before and compared to a site of tumor that had not been injected. Both of these sites shared as part of the clinical protocol an exposure to low-dose radiation (2 grays on each for two successive days). Single-cell suspensions were rested in the medium with no further exposure to CpG for 24 hours before analysis of OX40 expression by flow cytometry.

Statistical analysis

Prism software (GraphPad) was used to analyze tumor growth and to determine statistical significance of differences between groups by applying an unpaired Student's *t* test. *P* values <0.05 were considered significant. The Kaplan-Meier method was used for survival analysis. *P* values were calculated using the log-rank test (Mantel-Cox).

SUPPLEMENTARY MATERIALS

www.sciencetranslationalmedicine.org/cgi/content/full/10/426/eaan4488/DC1

Fig. S1. In situ vaccination with a TLR9 ligand induces the local expression of OX40 but not that of PD1 or CTLA4.

Fig. S2. CpG induces the expression of OX40 on CD4 T cells.

Fig. S3. Cytokines are playing a role in the CpG T cell cross-talk.
Fig. S4. Intracellular IFN-γ production of $CD4^+$ cells.
Fig. S5. Frequency of T cell subsets.
Fig. S6. Tumor recurrence is sensitive to treatment with anti-OX40 and CpG.
Fig. S7. Resiquimod (R848) in combination with anti-OX40 and anti-PD1/PDL1 in combination with CpG.
Fig. S8. In situ vaccination with CpG and anti-OX40 is effective against breast carcinoma, colon cancer, and melanoma.
Fig. S9. Dose de-escalation of CpG and αOX40 antibody.
Fig. S10. Systemic administration of anti-αOX40 antibody.
Fig. S11. Long-term memory in cured mice.
Fig. S12. Confirmation of T_{reg} depletion from the tumor.
Fig. S13. Anti-OX40 antibody stimulates T_{effs} and inhibits function of T_{regs}.
Fig. S14. Requirement for Fc competency of the anti-OX40 antibody.
Fig. S15. Neither T_{regs} nor T_{effs} are depleted by anti-OX40 antibody.
Table S1. Primary data.

REFERENCES AND NOTES

1. E. M. Sotomayor, I. Borrello, E. Tubb, F.-M. Rattis, H. Bien, Z. Lu, S. Fein, S. Schoenberger, H. I. Levitsky, Conversion of tumor-specific $CD4^+$ T-cell tolerance to T-cell priming through in vivo ligation of CD40. *Nat. Med.* **5**, 780–787 (1999).
2. K. Staveley-O'Carroll, E. Sotomayor, J. Montgomery, I. Borrello, L. Hwang, S. Fein, D. Pardoll, H. Levitsky, Induction of antigen-specific T cell anergy: An early event in the course of tumor progression. *Proc. Natl. Acad. Sci. U.S.A.* **95**, 1178–1183 (1998).
3. T. So, M. Croft, Cutting edge: OX40 inhibits TGF-beta- and antigen-driven conversion of naive CD4 T cells into $CD25^+Foxp3^+$ T cells. *J. Immunol.* **179**, 1427–1430 (2007).
4. M. D. Vu, X. Xiao, W. Gao, N. Degauque, M. Chen, A. Kroemer, N. Killeen, N. Ishii, X. C. Li, OX40 costimulation turns off $Foxp3^+$ Tregs. *Blood* **110**, 2501–2510 (2007).
5. J. D. Fontenot, J. P. Rasmussen, L. M. Williams, J. L. Dooley, A. G. Farr, A. Y. Rudensky, Regulatory T cell lineage specification by the forkhead transcription factor Foxp3. *Immunity* **22**, 329–341 (2005).
6. E. Y. Lin, J. G. Jones, P. Li, L. Zhu, K. D. Whitney, W. J. Muller, J. W. Pollard, Progression to malignancy in the polyoma middle T oncoprotein mouse breast cancer model provides a reliable model for human diseases. *Am. J. Pathol.* **163**, 2113–2126 (2003).
7. C. T. Guy, R. D. Cardiff, W. J. Muller, Induction of mammary tumors by expression of polyomavirus middle T oncogene: A transgenic mouse model for metastatic disease. *Mol. Cell. Biol.* **12**, 954–961 (1992).
8. T. Yamaguchi, K. Hirota, K. Nagahama, K. Ohkawa, T. Takahashi, T. Nomura, S. Sakaguchi, Control of immune responses by antigen-specific regulatory T cells expressing the folate receptor. *Immunity* **27**, 145–159 (2007).
9. K. Lahl, T. Sparwasser, In vivo depletion of $FoxP3^+$ Tregs using the DEREG mouse model. *Methods Mol. Biol.* **707**, 157–172 (2011).
10. K. Lahl, C. Loddenkemper, C. Drouin, J. Freyer, J. Arnason, G. Eberl, A. Hamann, H. Wagner, J. Huehn, T. Sparwasser, Selective depletion of $Foxp3^+$ regulatory T cells induces a scurfy-like disease. *J. Exp. Med.* **204**, 57–63 (2007).
11. K. S. Voo, L. Bover, M. L. Harline, L. T. Vien, V. Facchinetti, K. Arima, L. W. Kwak, Y. J. Liu, Antibodies targeting human OX40 expand effector T cells and block inducible and natural regulatory T cell function. *J. Immunol.* **191**, 3641–3650 (2013).
12. Y. Bulliard, R. Jolicoeur, J. Zhang, G. Dranoff, N. S. Wilson, J. L. Brogdon, OX40 engagement depletes intratumoral Tregs via activating FcγRs, leading to antitumor efficacy. *Immunol. Cell Biol.* **92**, 475–480 (2014).
13. F. Nimmerjahn, J. V. Ravetch, Fcγ receptors as regulators of immune responses. *Nat. Rev. Immunol.* **8**, 34–47 (2008).
14. F. Li, J. V. Ravetch, Inhibitory Fcγ receptor engagement drives adjuvant and anti-tumor activities of agonistic CD40 antibodies. *Science* **333**, 1030–1034 (2011).
15. D. Zhang, M. V. Goldberg, M. L. Chiu, Fc engineering approaches to enhance the agonism and effector functions of an anti-OX40 antibody. *J. Biol. Chem.* **291**, 27134–27146 (2016).
16. P. O. Krutzik, G. P. Nolan, Fluorescent cell barcoding in flow cytometry allows high-throughput drug screening and signaling profiling. *Nat. Methods* **3**, 361–368 (2006).
17. A. Burocchi, P. Pittoni, A. Gorzanelli, M. P. Colombo, S. Piconese, Intratumor OX40 stimulation inhibits IRF1 expression and IL-10 production by Treg cells while enhancing CD40L expression by effector memory T cells. *Eur. J. Immunol.* **41**, 3615–3626 (2011).
18. A. P. Vicari, C. Chiodoni, C. Vaure, S. Ait-Yahia, C. Dercamp, F. Matsos, O. Reynard, C. Taverne, P. Merle, M. P. Colombo, A. O'Garra, G. Trinchieri, C. Caux, Reversal of tumor-induced dendritic cell paralysis by CpG immunostimulatory oligonucleotide and anti–interleukin 10 receptor antibody. *J. Exp. Med.* **196**, 541–549 (2002).
19. C. Guiducci, A. P. Vicari, S. Sangaletti, G. Trinchieri, M. P. Colombo, Redirecting in vivo elicited tumor infiltrating macrophages and dendritic cells towards tumor rejection. *Cancer Res.* **65**, 3437–3446 (2005).
20. S. N. Gettinger, L. Horn, L. Gandhi, D. R. Spigel, S. J. Antonia, N. A. Rizvi, J. D. Powderly, R. S. Heist, R. D. Carvajal, D. M. Jackman, L. V. Sequist, D. C. Smith, P. Leming, D. P. Carbone, M. C. Pinder-Schenck, S. L. Topalian, F. S. Hodi, J. A. Sosman, M. Sznol, D. F. McDermott, D. M. Pardoll, V. Sankar, C. M. Ahlers, M. Salvati, J. M. Wigginton, M. D. Hellmann, G. D. Kollia, A. K. Gupta, J. R. Brahmer, Overall survival and long-term safety of nivolumab (anti–programmed death 1 antibody, BMS-936558, ONO-4538) in patients with previously treated advanced non-small-cell lung cancer. *J. Clin. Oncol.* **33**, 2004–2012 (2015).
21. D. F. McDermott, C. G. Drake, M. Sznol, T. K. Choueiri, J. D. Powderly, D. C. Smith, J. R. Brahmer, R. D. Carvajal, H. J. Hammers, I. Puzanov, F. S. Hodi, H. M. Kluger, S. L. Topalian, D. M. Pardoll, J. M. Wigginton, G. D. Kollia, A. Gupta, D. McDonald, V. Sankar, J. A. Sosman, M. B. Atkins, Survival, durable response, and long-term safety in patients with previously treated advanced renal cell carcinoma receiving nivolumab. *J. Clin. Oncol.* **33**, 2013–2020 (2015).
22. E. Gonzalez-Rodriguez, D. Rodriguez-Abreu; Spanish Group for Cancer Immuno-Biotherapy, Immune checkpoint inhibitors: Review and management of endocrine adverse events. *Oncologist* **21**, 804–816 (2016).
23. L. Kottschade, A. Brys, T. Peikert, M. Ryder, L. Raffals, J. Brewer, P. Mosca, S. Markovic; Midwest Melanoma Partnership, A multidisciplinary approach to toxicity management of modern immune checkpoint inhibitors in cancer therapy. *Melanoma Res.* **26**, 469–480 (2016).
24. A. Sgambato, F. Casaluce, P. C. Sacco, G. Palazzolo, P. Maione, A. Rossi, F. Ciardiello, C. Gridelli, Anti PD-1 and PDL-1 immunotherapy in the treatment of advanced non-small cell lung cancer (NSCLC): A review on toxicity profile and its management. *Curr. Drug Saf.* **11**, 62–68 (2016).
25. M. F. Fransen, T. C. van der Sluis, F. Ossendorp, R. Arens, C. J. M. Melief, Controlled local delivery of CTLA-4 blocking antibody induces $CD8^+$ T-cell–dependent tumor eradication and decreases risk of toxic side effects. *Clin. Cancer Res.* **19**, 5381–5389 (2013).
26. A. Marabelle, H. Kohrt, R. Levy, Intratumoral anti-CTLA-4 therapy: Enhancing efficacy while avoiding toxicity. *Clin. Cancer Res.* **19**, 5261–5263 (2013).
27. A. Marabelle, H. Kohrt, I. Sagiv-Barfi, B. Ajami, R. C. Axtell, G. Zhou, R. Rajapaksa, M. R. Green, J. Torchia, J. Brody, R. Luong, M. D. Rosenblum, L. Steinman, H. I. Levitsky, V. Tse, R. Levy, Depleting tumor-specific Tregs at a single site eradicates disseminated tumors. *J. Clin. Invest.* **123**, 2447–2463 (2013).
28. S. Piconese, B. Valzasina, M. P. Colombo, OX40 triggering blocks suppression by regulatory T cells and facilitates tumor rejection. *J. Exp. Med.* **205**, 825–839 (2008).
29. J. Ziai, G. Frantz, L. Zhang, C. Kozlowski, H. Gilbert, J. Smith, M. Kowanetz, J. M. Kim, M. Huseni, Prevalence analysis of OX40-positive cell populations in solid tumors. *J. Immunother. Cancer* **3** (suppl. 2), P113 (2015).
30. S. Mallett, S. Fossum, A. N. Barclay, Characterization of the MRC OX40 antigen of activated CD4 positive T lymphocytes—A molecule related to nerve growth factor receptor. *EMBO J.* **9**, 1063–1068 (1990).
31. K. Sugamura, N. Ishii, A. D. Weinberg, Therapeutic targeting of the effector T-cell co-stimulatory molecule OX40. *Nat. Rev. Immunol.* **4**, 420–431 (2004).
32. T. A. Triplett, C. G. Tucker, K. C. Triplett, Z. Alderman, L. Sun, L. E. Ling, E. T. Akporiaye, A. D. Weinberg, STAT3 signaling is required for optimal regression of large established tumors in mice treated with anti-OX40 and TGFβ receptor blockade. *Cancer Immunol. Res.* **3**, 526–535 (2015).
33. K. A. Murphy, M. G. Lechner, F. E. Popescu, J. Bedi, S. A. Decker, P. Hu, J. R. Erickson, M. G. O'Sullivan, L. Swier, A. M. Salazar, M. R. Olin, A. L. Epstein, J. R. Ohlfest, An in vivo immunotherapy screen of costimulatory molecules identifies Fc-OX40L as a potent reagent for the treatment of established murine gliomas. *Clin. Cancer Res.* **18**, 4657–4668 (2012).
34. S. Murata, B. H. Ladle, P. S. Kim, E. R. Lutz, M. E. Wolpoe, S. E. Ivie, H. M. Smith, T. D. Armstrong, L. A. Emens, E. M. Jaffee, R. T. Reilly, OX40 costimulation synergizes with GM-CSF whole-cell vaccination to overcome established $CD8^+$ T cell tolerance to an endogenous tumor antigen. *J. Immunol.* **176**, 974–983 (2006).
35. A. Curti, M. Parenza, M. P. Colombo, Autologous and MHC class I–negative allogeneic tumor cells secreting IL-12 together cure disseminated A20 lymphoma. *Blood* **101**, 568–575 (2003).
36. A. Song, J. Song, X. Tang, M. Croft, Cooperation between CD4 and CD8 T cells for anti-tumor activity is enhanced by OX40 signals. *Eur. J. Immunol.* **37**, 1224–1232 (2007).
37. D. Hirschhorn-Cymerman, S. Budhu, S. Kitano, C. Liu, F. Zhao, H. Zhong, A. M. Lesokhin, F. Avogadri-Connors, J. Yuan, Y. Li, A. N. Houghton, T. Merghoub, J. D. Wolchok, Induction of tumoricidal function in $CD4^+$ T cells is associated with concomitant memory and terminally differentiated phenotype. *J. Exp. Med.* **209**, 2113–2126 (2012).
38. M. J. Gough, C. E. Ruby, W. L. Redmond, B. Dhungel, A. Brown, A. D. Weinberg, OX40 agonist therapy enhances CD8 infiltration and decreases immune suppression in the tumor. *Cancer Res.* **68**, 5206–5215 (2008).
39. N. Kitamura, S. Murata, T. Ueki, E. Mekata, R. T. Reilly, E. M. Jaffee, T. Tani, OX40 costimulation can abrogate $Foxp3^+$ regulatory T cell-mediated suppression of antitumor immunity. *Int. J. Cancer* **125**, 630–638 (2009).

40. B. Valzasina, C. Guiducci, H. Dislich, N. Killeen, A. D. Weinberg, M. P. Colombo, Triggering of OX40 (CD134) on $CD4^+CD25^+$ T cells blocks their inhibitory activity: A novel regulatory role for OX40 and its comparison with GITR. *Blood* **105**, 2845–2851 (2005).
41. R. G. Lapidus, S. J. Nass, N. E. Davidson, The loss of estrogen and progesterone receptor gene expression in human breast cancer. *J. Mammary Gland Biol. Neoplasia* **3**, 85–94 (1998).
42. S. Ménard, E. Tagliabue, M. Campiglio, S. M. Pupa, Role of HER2 gene overexpression in breast carcinoma. *J. Cell. Physiol.* **182**, 150–162 (2000).
43. J. E. Maglione, D. Moghanaki, L. J. T. Young, C. K. Manner, L. G. Ellies, S. O. Joseph, B. Nicholson, R. D. Cardiff, C. L. MacLeod, Transgenic Polyoma middle-T mice model premalignant mammary disease. *Cancer Res.* **61**, 8298–8305 (2001).

Funding: This work is supported by grants from the NIH (R01 CA188005), the Leukemia and Lymphoma Society (TAP-120921), and the Boaz and Varda Dotan and the Phil N. Allen foundations. **Author contributions:** I.S.-B., D.K.C., I.S.A., and A.T.M. designed and performed all experiments. I.S.-B., S.L., S.S.G., and R.L. wrote the paper. **Competing interests:** S.S.G. is founder and equity holder of CellSight Inc. that develops and translates multimodality strategies for imaging cell trafficking/transplantation. All other authors declare that they have no competing interests. **Data and materials availability:** CpG SD-101 is available from Dynavax Technologies under a material transfer agreement.

Submitted 13 April 2017
Resubmitted 13 September 2017
Accepted 13 December 2017
Published 31 January 2018
10.1126/scitranslmed.aan4488

Citation: I. Sagiv-Barfi, D. K. Czerwinski, S. Levy, I. S. Alam, A. T. Mayer, S. S. Gambhir, R. Levy, Eradication of spontaneous malignancy by local immunotherapy. *Sci. Transl. Med.* **10**, eaan4488 (2018).

Science Translational Medicine

Eradication of spontaneous malignancy by local immunotherapy

Idit Sagiv-Barfi, Debra K. Czerwinski, Shoshana Levy, Israt S. Alam, Aaron T. Mayer, Sanjiv S. Gambhir and Ronald Levy

Sci Transl Med **10**, eaan4488.
DOI: 10.1126/scitranslmed.aan4488

Deliver locally, act globally

Mobilizing endogenous T cells to fight tumors is the goal of many immunotherapies. Sagiv-Barfi *et al*. investigated a combination therapy in multiple types of mouse cancer models that could provide sustainable antitumor immunity. Specifically, they combined intratumoral delivery of a TLR9 ligand with OX40 activation to ramp up T cell responses. This dual immunotherapy led to shrinkage of distant tumors and long-term survival of the animals, even in a stringent spontaneous tumor model. Both of these stimuli are in clinical trials as single agents and could likely be combined at great benefit for cancer patients.